remote sensing

MDPI

Technical Note

Performance Evaluation of China's First Ocean Dynamic Environment Satellite Constellation

Dan Qin [1,2], Yongjun Jia [1,*], Mingsen Lin [1] and Shanwei Liu [2]

[1] National Satellite Ocean Application Service, Beijing 100081, China
[2] College of Oceanography and Space Informatics, China University of Petroleum, Qingdao 266058, China
* Correspondence: jiayongjun@mail.nsoas.org.cn

Abstract: China's first dynamic environment satellite constellation includes the HY-2B, HY-2C, and HY-2D satellites. In this study, the along track SLA, SWH, and SSWS of this satellite constellation were evaluated. SLA parameters are evaluated using self-crossing and dual-crossing methods. The SSWS and SWH data were evaluated by comparing with NDBC buoy and other available satellites' data. The evaluation revealed that the standard deviation of the SLA from the HY-2B/C/D satellites' single mission crossovers was 3.29 cm, 3.51 cm, and 3.72 cm, respectively. In addition, at the dual-crossovers of the Jason-3 satellite and the HY-2B satellite, the HY-2B satellite, and the HY-2C/D satellites, the standard deviation was determined to be 3.40 cm, 3.48 cm, and 4.25 cm, respectively. The accuracy of the SWH products of the HY-2B/C/D satellite radar altimeters was observed to be 0.23 m, 0.25 m, and 0.26 m, respectively. The accuracy of the SSWS data of the HY-2B/C/D satellite radar altimeters was observed to be 1.48 m/s, 1.59 m/s, and 1.35 m/s, respectively. In addition, this study also analyzed and compared the observation efficiency of the dynamic environment satellite constellation with the following six satellites: Sentinel-3(A, B), Jason-3, Sentinel-6A, Saral, and Cryosat-2. Observation efficiency refers to selection of any point on the globe to find a minimum radius of at least one observation point within a circle in a 14-day period. The analysis results demonstrated that observation efficiency of China's first dynamic environment satellite constellation was comparable to that of the six satellites.

Keywords: dynamic environment satellite constellation; validation; SLA; SWH; SSWS; HY-2

Citation: Qin, D.; Jia, Y.; Lin, M.; Liu, S. Performance Evaluation of China's First Ocean Dynamic Environment Satellite Constellation. *Remote Sens.* **2023**, *15*, 4780. https://doi.org/10.3390/rs15194780

Academic Editors: Chung-Ru Ho and Andrea Storto

Received: 10 July 2023
Revised: 22 September 2023
Accepted: 25 September 2023
Published: 30 September 2023

1. Introduction

In 2021, China built the first ocean dynamic environment satellite constellation, which included the HY-2B, HY-2C, and HY-2D ocean dynamic environment satellites. The HY-2B satellite is a sun-synchronous orbit satellite equipped with a radar altimeter, a scatterometer, a radiometer, a correction radiometer, a data collection system, and an automatic ship identification system. HY-2B has a 14-day repeat cycle. The HY-2C and HY-2D satellites are non-sun-synchronous orbit satellites with an inclination of 66°. They are equipped with all payloads same as HY-2B except the radiometer and have repeat cycles of 10 days. The satellite radar altimeter is the main payload of China's ocean dynamic environment satellite constellation. Table 1 details the main information of China's first ocean dynamic environment satellite constellation (https://osdds.nsoas.org.cn, accessed on 23 September 2023).

The calibration and validation of the altimeter data were critical steps in the altimetry mission. Accurate and objective calibration and validation can provide reliable information and assurance to the users of the data products. Jia et al. [1] evaluated the quality of the sea surface height (SSH), significant wave height (SWH), and SSWS data products using cross-calibration of HY-2B radar altimeter data with the Jason-3 data. It was concluded that the HY-2B altimeter data products had good stability and high accuracy. In addition, the quality of the HY-2B SWH products is evaluated by comparing with the SWH obtained from NDBC buoys and Jason-2/Jason-3 satellite altimeters. Their root-mean-squared error

was 27 cm, 26 cm, and 23 cm, respectively [2]. Therefore, the comparison results confirmed that the SWH data of the HY-2B are of higher quality. To assess the data quality and the performance of the altimeter systems, the data from the Jason-1 [3–5], Jason-2, Envisat [6], and SARAL/Altika satellites [7,8] were calibrated and validated using a cross-calibration approach. Meng et al. [9] used the Geophysical Data Records (GDR) of HY-2B and Jason-3 satellites observed during the same period as a reference, and quality analysis was conducted on the SSWS data in HY-2C satellite Sensor Geophysical Data Records (SGDR). The average difference in SLA at the dual-crossover point of HY-2C satellite SGDR data and HY-2B satellite and Jason 3 satellite GDR data is −0.47 cm and −0.3 cm, respectively, with standard deviations of 5.32 cm and 5.32 cm. These data indicate that the height measurement accuracy of HY-2C satellite is consistent with that of HY-2B satellite and Jason 3 satellite. Yang et al. [10] evaluated the data quality of the SSWS product and carried out by the HY-2D satellite Ku-band scatterometer. SSWS observed by the scatterometer (HSCAT-D) were validated by comparing with wind data from the U.S. National Data Buoy Center (NDBC) buoys and European Centre for Medium-Range Weather Forecasts (ECMWF) model. The statistical results show that the HSCAT-D winds have a good agreement with the buoys' wind measurements, and in comparison with buoy winds, the wind speed standard deviation (STD) and root-mean-squared errors (RMSE) of direction were 0.78 m/s and 14.10°, respectively. In previous studies, only the accuracy of mono-mission satellite radar altimeter data was evaluated, and the accuracy of the satellite constellation was not comprehensively and systematically evaluated. The full elements (SWH, SLA, and SSWS) of the HY-2C/D satellites radar altimeter GDR data have not been verified. The difference between this article and previous articles is that the validation parameters are different, and the validation data category and the satellite payload are different. In this study, the quality levels of the HY-2B/C/D satellites' along-track SLA, SWH, and SSWS data were validated as a whole in order to perform a comprehensive and systematic evaluation. A comprehensive and systematic evaluation of the altimetry data of the HY-2B/C/D three satellite radar altimeters includes the observation efficiency of the altimeter and the observation accuracy of the observation parameters SLA, SSWS, and SWH.

Table 1. Composition of China's ocean dynamic environment satellite constellation and its main information.

Satellite	HY-2B	HY-2C/D
Track height/km	970.732/972.836 km	957.583/958.490 km
Repeat cycle/day	14/168 day	10/400 day
Instruments	Radar altimeter, microwave scatterometer, microwave radiometer, calibration radiometer, automatic identification system (AIS) for ships, data collection system (DCS)	Radar altimeter, microwave scatterometer, calibration radiometer, automatic ship identification system (AIS), data collection system (DCS)
Localization	Sun-synchronous, frozen orbit	Non-sun-synchronous orbit with the inclination of 66°, frozen track
Measurement elements	Sea surface wind field, sea surface height, SWH, gravity field, ocean circulation, sea surface temperature	Sea surface wind field, sea surface height, SWH, gravity field, ocean circulation, sea surface temperature

In this study, Section 2 introduces the data acquisition and ocean data screening criteria and the basic methods used for the experiments. Section 3 discusses the efficiency levels of the three HY-2B/C/D satellites and radar altimeter observations of six other satellites are compared and analyzed. The standard deviation of the SLA at the single mission

crossover points and the dual crossover points for each cycle of the HY-2B/C/D satellites was calculated. Section 4 discusses and summarizes the article.

2. Data and Methods

2.1. Data Products

The Geophysical Data Records (GDR) of the HY-2B/C/D satellites, which were available from the National Satellite Ocean Application Service (https://osdds.nsoas.org.cn, accessed on 23 September 2023), were examined for validation in the current study. Considering that the ocean dynamic environment satellite constellation was built after the launch of the HY-2D satellite, the data time frame was from 24 May 2021 to 27 May 2022. The HY-2B altimeter GDR data included Cycle 68 to Cycle 93. The HY-2C altimeter GDR data included Cycle 25 to Cycle 62, and the HY-2D altimeter GDR data included Cycle 01 to Cycle 37.

The Jason-3 altimeter GDR data are used in this study as the comparison for Cycle 195 to Cycle 303, which correspond to the time range of 25 May 2021 to 28 May 2022. The Jason-3 data version was Version F.

This study evaluated the global observation efficiency using data collected from Seninel-3A, Seninel-3B, Seninel-6A, Cryosat-2, Saral, and HY-2B/C/D satellites from 1 January 2022 to 14 January 2022. The complete products of Seninel-3A and Seninel-3B contain three NetCDF files, namely, reduced measurement, standard measurement, and enhanced measurement data. The study used the standard measurement data of the SRAL product. In addition, the Cryosat-2 Level-2 GDR (https://science-pds.cryosat.esa.int, accessed on 23 September 2023) and Saral GDR (http://www.aviso.altimetry.fr, accessed on 23 September 2023) satellite altimetry data were used to calculate the observation efficiency of multiple satellites. The data from Seninel-3A, Seninel-3B, and Seninel-6A were shared by EUMETSAT through Copernicus Online Data Access (https://www.eumetsat.int, accessed on 23 September 2023).

In this study, NDBC buoy data from 1 January 2021 to 31 May 2022 were provided by the National Data Buoy Center (https://www.ndbc.noaa.gov, accessed on 23 September 2023). The NDBC dataset has been extensively utilized for model validations and satellite system calibrations [11]. In addition, to avoid the influence effects of land (as well as islands), only data from buoys located more than 50 km offshore and at water depths greater than 1000 m were selected in the study conducted.

2.2. Methods

Theoretically speaking, the satellite radar altimeter data and NDBC buoy data will overlap in time and space when compared for verification purposes. However, it is seldom possible to achieve this ideal situation. Therefore, it is necessary to select radar altimeter data with small temporal and spatial differences when adopting buoy data for calculation purposes. When evaluating SWH and SSWS, the spatio-temporal windows selected in the current study were 50 km and 30 min. In the other words, the spatial separation between the satellite altimeter data and the buoy data in the matched data was no more than 50 km, and the time interval was no more than 30 min. These spatio-temporal matching criteria have been widely used in many previous studies [12–14].

The cross-calibration with other missions detected any instrument drifts or inter-mission bias, which was essential to obtain consistent multi-satellite datasets [15]. For a single satellite or multiple satellites with the same trajectory, the intersection point of the ground trajectory is the only intersection point of the ascending and descending track, known as the self-crossover point. The intersection point of the ground trajectories of two satellites with different trajectories may be either the crossover point of ascending and descending track, or the crossover point of both ascending and descending track, known as the dual crossover point. The determination of satellite intersection points is divided into two steps: determining the approximate position and determining the precise position based on the approximate position. Preliminary screening of two trajectories with

intersections, using the least squares method to perform quadratic polynomial fitting on satellite trajectories, calculating undetermined coefficients, and then, establishing a system of equations to obtain the approximate location of the intersection (φ_i, λ_i) [16–22] (Figure 1).

$$\begin{aligned} \varphi_i &= A_a\lambda_i^2 + B_a\lambda_i + C_a \\ \varphi_i &= A_d\lambda_i^2 + B_d\lambda_i + C_d \end{aligned} \quad (1)$$

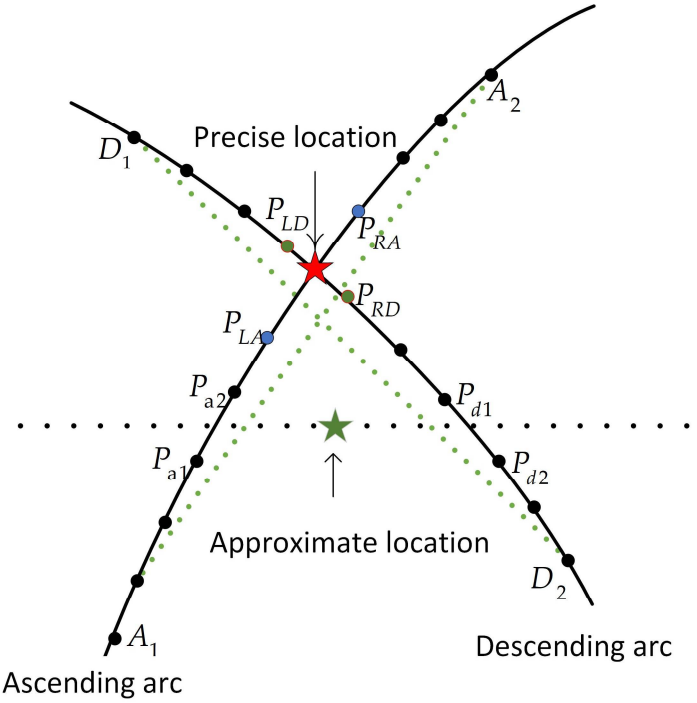

Figure 1. Schematic diagram for determining the location of intersections.

Using the approximate latitude obtained as a reference, select the 10 closest points to the reference latitude in the ascending segment to form a new ascending arc segment. In the descending segment, select the 10 closest points to the reference latitude to form a new descending arc segment. The intersection point of the two arc segments is the required accurate position.

The findings of a previous study were referenced [23], and the radar altimeter performances were evaluated using the following four parameters: root-mean-squared error (RMSE); correlation coefficient (R); mean deviation (Bias); and standard of deviation (STD).

3. Results

3.1. Observational Effectiveness Assessment of the HY-2B/C/D Satellite Constellation

The study analyzed the observation efficiency of HY-2B/C/D satellites, in comparison with six other satellite systems, including Sentinel-3(A, B), Jason-3, Sentinel-6A, Cryosat-2, and Saral. The comparison was conducted using nine satellites' altimetry data, and the observation efficiency was to search for the minimum radius of at least one observation point within a circle at any point on Earth within a 14-day period. The study then plotted the variations of that radius in an observation period of 1 to 14 days, which represented the observational effectiveness of China's first dynamic environment satellite constellation.

The study analyzed the observation efficiency separately for the six satellites that are not Chinese, as well as the total nine satellites. The study aimed to illustrate the observation efficiency of the HY-2B/C/D constellation, which has achieved all-day, all-weather monitoring capabilities, including SSH, SWH, and other ocean dynamic environmental elements.

As can be seen in Figure 2, the minimum radius to find the observation point on the global ocean surface shrank from 471.12 km to 90.33 km in the 14-day cycle, where the

HY-2C/D cycle was 10 days, and the HY-2C/D were repeat tracked from 11 to 14 days. The observation efficiency of the first nine days was slightly lower compared for the six non-Chinese satellites. However, from the 9th day onward, the observation efficiency of the HY-2B/C/D network was higher than the six other satellites' observational effectiveness. Furthermore, it was determined from the overall observation efficiency of the nine satellites that the observation efficiency on the second day was quite obvious, and the minimum radius to find the observation point within 14 days was 59.52 km. Overall, the observation efficiency level of China's first dynamic environment satellite constellation was high. Therefore, the network has the ability to provide services for the safety of marine vessel navigation, marine disaster prevention and mitigation, and marine resource investigations.

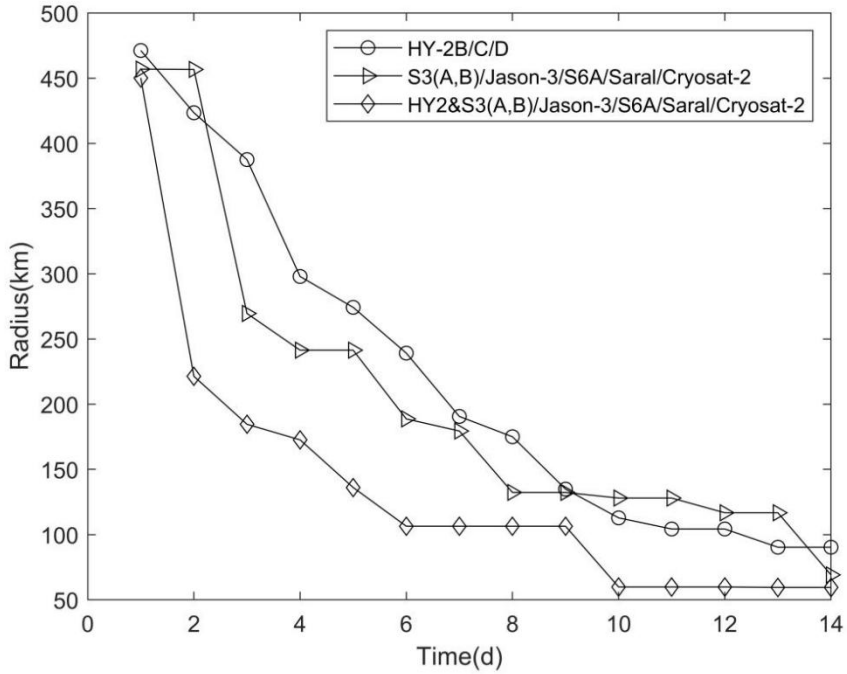

Figure 2. Observation efficiency of the HY-2B/C/D satellite network.

3.2. Sea-Level Performances

The purpose of this study is to verify and evaluate the performance of HY-2B/C/D three satellites, which required the evaluations of the relevant parameters of the Level 2 products of all three satellites (Table 2), and the specific link is as follows: https://osdds.nsoas.org.cn, accessed on 23 September 2023.

Table 2. HY-2B/C/D satellite data screening criteria.

Parameter	Min	Max
range_numval_ku	10	-
range_rms_ku	0 m	0.2 m
model_dry_tropo_corr	−2.5 m	−1.9 m
rad_wet_tropo_corr	−0.5 m	−0.001 m
iono_corr_alt_k	−0.4 m	0.04 m
sea_state_bias_ku	−0.5 m	0 m
ocean_tide_sol1	−5 m	5 m
solid_earth_tide	−1 m	1 m

Table 2. *Cont.*

Parameter	Min	Max
pole_tide	−0.15 m	0.15 m
swh_ku	0 m	11 m
sig0_ku	7 db	30 db
altimeter wind speed	0 m/s	30 m/s
off_nadir_angle_ku_wvf	-0.2 deg^2	0.64 deg^2
sig0_rms_ku	-	1 db
sig0_numval_ku	10	-
alt_range_ku	−130 m	100 m

The SLA was calculated as follows, where the mean sea surface of the HY-2B satellite is mss_cnes_cls2015. The specific link is as follows: https://www.aviso.altimetry.fr/en/data/products/auxiliary-products/mss.html, accessed on 23 September 2023.

$$\text{SLA} = \text{Altitude} - (\text{Altimeter Range} + \sum \text{Corrections}) - \text{Mean Sea Surface} \quad (2)$$

One of the formulae is as follows: ΣCorrections = Model Dry Troposphere Correction + Radiometer Wet Tropospheric Correction + Sea State Bias correction + Inverted Barometer Height Correction + HF Fluctuations of Sea Surface Topography + Solid Earth Tide Height Correction + Pole Tide Height.

The correction of dry delay and atmospheric humidity on satellite radar altimeter signal is achieved through the use of the model dry troposphere correction parameter and radiometer wet tropospheric correction parameter. Sea state bias correction parameter is used to correct for the influence of sea surface topography on the signal. Ionospheric barometer height correction parameter is used to correct for the influence of ionospheric electron density on the signal. HF fluctuations of sea surface topography parameter is used to correct high-frequency change in the shape of the sea surface. The solid earth tide height correction parameter and pole tide parameter are used to correct the influence of earth's solid tide elevation and polar tide elevation.

3.2.1. Self-Crossing Point Analysis

The ideal situation would be if the mean differences in the SLA at the self-crossing points were close to zero, and the standard deviation was very small. In this study, the GDR data were screened according to HY-2B data screening criteria. The time range of the HY-2B/C/D satellites' ascending and descending tracks to determine the self-crossing points was three days. In order to achieve assessments with high accuracy, the data were analyzed using the following criteria: between 50° of the equator north and south latitudes, water depth greater than 1000 m, and SLA lower than 20 cm [24].

It can be seen in Figure 3 that the standard deviation of the SLA at the self-crossing points for each cycle of the satellite were 3.30 cm, 3.51 cm, 3.72 cm, which indicated that the accuracy of HY-2B altimetry data was high and stable. HY-2C/D data gradually stabilized as the number of cycles increased.

3.2.2. Cross-Calibration with Multiple Satellite Systems

The Jason-3 satellite is the successor mission to the OSTM/Jason-2 satellite and is mainly used to study ocean circulations and sea surface height variability with high accuracy calibrations. The data from the Jason-3 satellite have been used as references to validate other altimeter data. This analysis of the GDR data of the Jason-3 satellite were used to verify the quality of the HY-2B SLA data. The HY-2B data period was utilized as a reference, and the cross-calibration of the HY-2B and Jason-3 data was analyzed. As detailed in Figure 4, the mean value of the standard deviation of the SLA differences at the dual-crossovers points of the HY-2B and Jason-3 satellites was 3.40 cm, with the maximum standard deviation of 3.61 cm for the data of Cycle 75. The data of the remainder of the

cycles were stable (between 3.30 cm and 3.50 cm). The standard deviation of the SLA at the dual-crossovers points of HY-2B and Jason-3 was found to be consistent with the SLA from the self-crossing points recorded by the HY-2B satellite altimeter. These findings reconfirm that the observations from the radar altimeter of the HY-2B satellite are stable and that the accuracy of this product is consistent with that of the Jason-3.

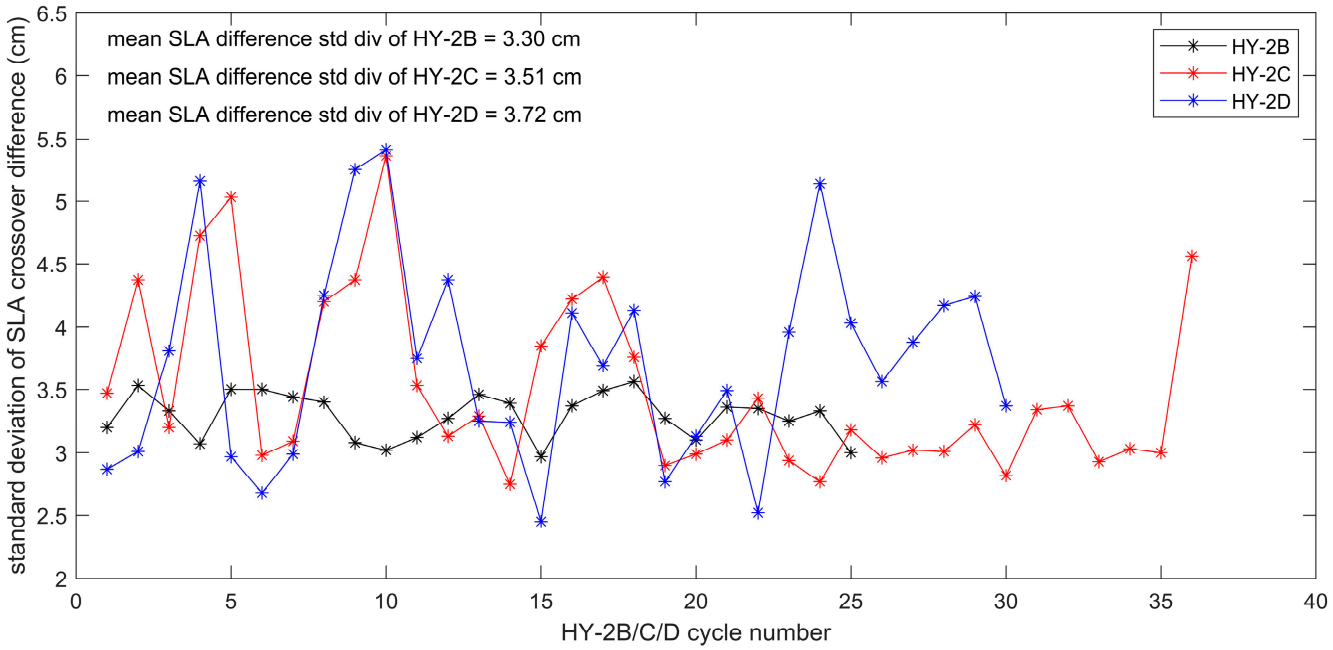

Figure 3. Cycle-by-cycle distributions of the sea level anomaly (SLA) differences at the mono-mission crossovers of the HY-2B/C/D satellite.

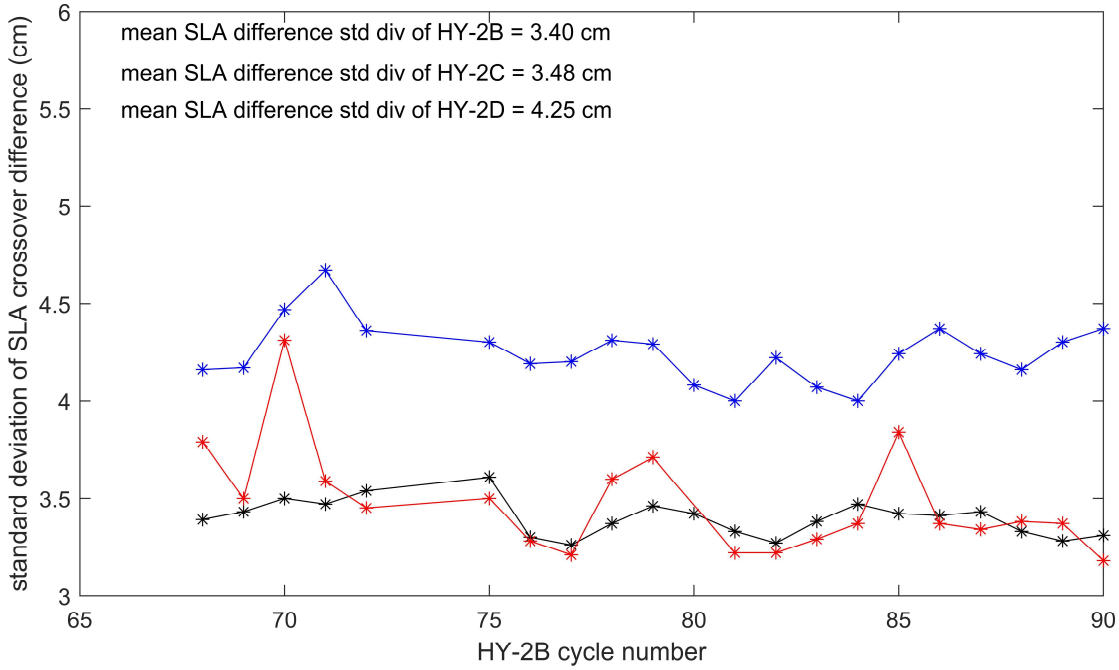

Figure 4. Cycle-by-cycle distributions of the sea level anomaly (SLA) differences at the crossover points of HY-2B and Jason-3 and HY-2B and HY-2C/D satellites (black line: HY-2B; red line: HY-2C; blue line: HY-2D).

The HY-2C, HY-2D, and Jason-3 have inclined orbits, with orbital inclination of 66°. The orbits of the three satellites are almost parallel, with a small number of crossover points in the low-latitude regions. Jason-3 cannot be used to evaluate HY-2C/D. The HY-2B altimetry data were determined to be of higher quality. Therefore, the HY-2B data can be used to verify the quality of HY-2C and HY-2D altimetry data.

As detailed in Figure 4, the HY-2B and HY-2C/D track crossover points of the SLA differences' standard deviation had an average value of 3.48 cm and 4.25 cm. Except for one cycle with large discrepancy, the data quality of HY-2C is high and the data are stable. The SLA measured by HY-2D showed some deviation from HY-2B data, possibly due to differences in the orbit determination methods used for the two satellites.

3.3. Significant Wave Height (SWH) Verification

The SWH is one of the three basic parameters of altimeter measurements. The SWH information is obtained from the waveforms returned by a radar altimeter [17,18,25,26]. SWH is estimated from the slope of the leading edge of the return pulse [26–30]. Many studies have been devoted to the validations of SWH data from TOPEX/Poseidon (T/P), Jason-1, Jason-2, ERS, and GEOSAT follow-up data and envisioned altimeters [31–34].

The quality of the three HY-2B/C/D satellites' SWH data was verified using NDBC buoy data and dual crossover point data between different satellites. In this study, the spatio-temporal matching required that the closest distance of the satellite nadir point from a buoy was less than 50 km, and the minimum observation time differences was 30 min [16,35]. The HY-2B/C/D SWH data were evaluated by analyzing the SWH differences values at the crossover points.

3.3.1. Comparison SWH with the Buoy Data

In this study, fifty NDBC buoys with water depths greater than 1000 m were used to assess the quality of the HY-2B/C/D satellites' SWH data. In this study, there are 354, 389, and 197 matching points between NDBC buoys and HY-2B/C/D at less than 50 km apart within 30 min, respectively. The spatial distribution of the buoys is shown in Figure 5.

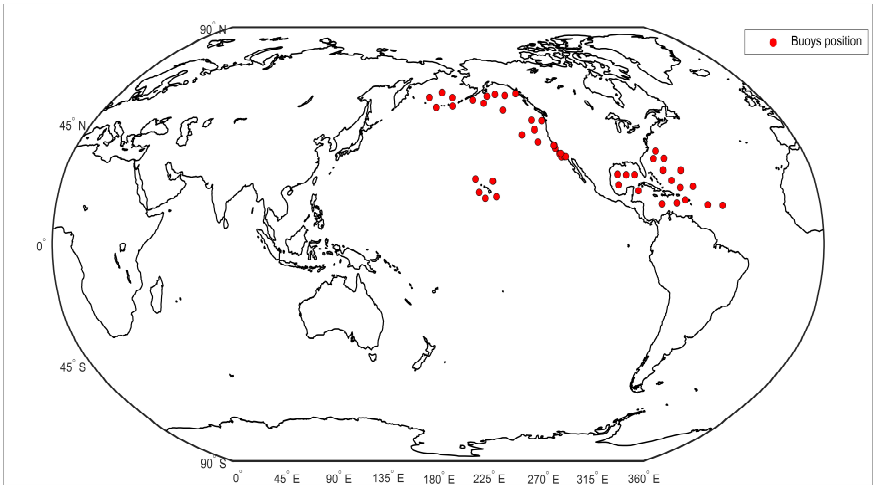

Figure 5. Positional distribution of the buoys.

As shown in Table 3, the SWH measurements of the HY-2B, HY-2C, and HY-2D satellites had deviations. The average deviation of the HY-2B/C/D SWH were 0 m, −0.02 m, and 0.15 m, respectively. The root-mean-squared errors were 0.23 m, 0.25 m, and 0.30 m, respectively, with standard deviation of 0.23 m, 0.25 m, and 0.26 m, respectively. The NDBC buoy data are an important reference to evaluate the SWH from the radar altimeters, and the results show that the SWH data from the three satellite radar altimeters are in good agreement with the buoy data.

Table 3. HY-2B/C/D satellite SWH data verification.

SWH	N	RMSE (m)	STD (m)	R	Mean SWH Div (m)
HY-2B/NDBC	354	0.23	0.23	0.99	0
HY-2C/NDBC	389	0.25	0.25	0.98	−0.02
HY-2D/NDBC	197	0.30	0.26	0.99	0.15
HY-2B/Jason-3	1052	0.17	0.17	0.99	0
HY-2C/HY-2B	1077	0.15	0.14	0.99	−0.06
HY-2D/HY-2B	758	0.30	0.25	0.99	0.17

The data of SWH < 0.5 m in altimeter data are generally not accurate enough, and similarly, when SWH is greater than 8 m, which is a giant wave, there are errors in the measurement, so the reliability of the data is somewhat controversial. In the validation of SWH, there was no significant difference between the HY-2B/D data and the NDBC matched data pairs. The data quality of HY-2B/D was stable and consistent. For HY-2C, this study recalculates the relevant parameters after excluding the three pairs of data with large differences, where the correlation coefficient is 0.9832 and the linear relationship between them is $SWH_{NDBC} = 0.9415 \times SWH_{HY-2C} + 0.1122$.

3.3.2. Comparison of SWH among Multiple Satellites

This study validated the HY-2B satellite's SWH data quality using Jason-3 satellite data. There were 1052 spatio-temporal matched points. As can be seen in Table 3, the mean deviation, standard deviation, and root-mean-squared error of the cross points were −0.0028 m, 0.17 m, and 0.17 m, respectively. The SWH measurements in the HY-2B Ku band were slightly higher than those of the Jason-3. However, there was significant agreement between the SWH of the HY-2B and Jason-3 satellites.

This study used the HY-2B data to verify the quality of the HY-2C and HY-2D SWH data. Table 3 shows the spatial and temporal matching of 1077 and 758 points, respectively, with mean deviation of −0.06 m and 0.17 m and standard deviation of 0.14 m and 0.25 m, respectively. The densest points were concentrated in the SWH of 1 to 6 m, and the numbers of SWH for the 0.5 to 1 m and 7 to 10 m ranges were minimal. The differences between the SWH became larger as the SWH values increased. There is a significant agreement between the SWH of HY-2B and HY-2C/D satellites. In addition, the quality of the HY-2C satellite's SWH data was higher than that of the HY-2D satellite.

3.4. Sea Surface Wind Speed (SSWS) Verification

The normalized backscatter coefficients of sea surface can be obtained by satellite radar altimeter, and the backscatter coefficients are related to the sea surface roughness [35]. Since wind is the main factor affecting the sea surface roughness, a geophysical mode function can be established for the interrelationship between the backscatter coefficients and the SSWS, and this model function can be used to invert the wind speeds from the observed backscatter coefficients measured by satellite altimeters [28,36]. The process of SSWS data verification in the study was consistent with the verification of SWH data, with the verification of SSWS based on the obtained buoy data and the multiple satellites tracking of dual-crossover points for the SSWS.

3.4.1. Comparison of SSWS with the Buoy Data

In this study, the same spatio-temporal matching method as the SWH verification was used to match 842, 1053, and 494 points, respectively. The mean deviation of HY-2B, HY-2C, and HY-2D satellites' wind speed data was −0.05 m/s, 0.95 m/s, and −0.52 m/s, respectively, with root-mean-squared errors of 1.48 m/s, 1.85 m/s, and 1.45 m/s, and standard deviation of 1.48 m/s, 1.59 m/s, and 1.35 m/s, respectively. Therefore, there was found to be significant agreement between the SSWS of HY-2B/C/D satellite network and the buoy data. Based on the above data, it was determined that the wind speed data of

the HY-2B and HY-2C satellites were of high quality. However, the HY-2D satellite had matched the least number of NDBC data. The densest matching was concentrated in the wind speed range of 3 to 15 m/s. The number of SSWS matches beyond 15 m/s was low.

The NDBC buoy data used in this paper have been calibrated. Anemometer heights on NDBC buoys vary according to buoy type. Anemometers on 3 m discus and 6 m NOMAD buoys are located approximately 5 m above the waterline. Anemometers on 10 and 12 m buoys are located 10 m above the waterline. Anemometer heights at CMAN stations vary widely, depending on site structure and elevation above sea level. NDBC adjusts wind speeds to conform to the universally accepted reference standard of 10 m. This is conducted to provide marine forecasters and data modelers a means to directly compare buoy observations with ship observations. This is one of the reasons why there is a discrepancy between the altimeter wind speed data and the NDBC buoy data.

3.4.2. Comparison of SSWS among Multiple Satellites

The standard deviation of the SSWS differences between the Jason-3 and HY-2B satellites' dual-crossover points was used to verify the HY-2B satellite's wind speed data. Table 4 shows that there were 693 points that satisfied the condition under the restrictions of a 30 min time range of a 50 km spatial range. The standard deviation of the SSWS differences at the dual-crossover points was determined to be 0.85 m/s, and the SSWS were concentrated between 3 and 15 m/s. The results of SSWS comparison between HY-2B and Jason-3 satellites showed that the SSWS obtained by Jason-3 satellite was slightly larger than that obtained by HY-2B satellite. However, we found a good agreement between these two satellites.

Table 4. HY-2B/C/D satellites' SSWS data verification.

SSWS	N	RMSE (m/s)	STD (m/s)	R	Mean SWH Div (m/s)
HY-2B/NDBC	842	1.48	1.48	0.92	−0.05
HY-2C/NDBC	1053	1.85	1.59	0.89	0.95
HY-2D/NDBC	494	1.45	1.35	0.95	−0.52
HY-2B/Jason-3	693	1.07	0.85	0.97	−0.66
HY-2C/HY-2B	948	1.27	0.95	0.97	0.85
HY-2D/HY-2B	722	1.16	1.13	0.96	−0.25

In line with the verification of the SWH data, this study used the HY-2B satellite's SSWS data to verify the HY-2C/D altimeter SSWS data. Table 4 shows that the HY-2B satellite and the HY-2C/D satellites had 948 and 722 dual-crossover points on their tracks, respectively, with a standard deviation of 0.95 m/s and 1.13 m/s, respectively. The quality of the HY-2C satellite's wind speed data was somewhat higher than that of the HY-2D satellite altimeter.

4. Discussion

In past studies, only one or both of the altimetry parameters were usually evaluated. However, in this study, the SLA, SWH, and SSWS of the HY-2B/C/D satellite were systematically evaluated, and the evaluation of all elements was realized, demonstrating the accuracy consistency between the three satellites. The standard deviation of the SLA between HY-2B and Jason-3 satellites at the dual-crossovers is less than 4 cm with good results, which shows that the data quality of HY-2B is more stable with high accuracy, and it is similar to the international equivalent satellite radar altimeter of Jason-3 satellite. Therefore, HY-2B altimetry data can be used to verify the SWH and SSWS data of HY-2C/D quality. The validation results of the self-crossing SLA data demonstrate that the accuracy of the HY-2D satellite's height measurement data is somewhat different from that of HY-2B/C satellites. The validation time interval is located in the early launch stage of the HY-2D satellite, and the observation data is unstable and missing. The standard deviation of multiple cycles of the dual-crossing SLA data is 4.25 cm, which is significantly different

from the standard deviations of 3.40 cm and 3.48 cm of the other two satellites' SLA data. It is hypothesized that the large bias in the HY-2D radar altimeter data is not significantly related to the inversion method, but to the instrument itself. Therefore, in the next version of this product, this study suggests addressing the relevant corrections. The accuracy levels of the SWH data products of the HY-2B/C/D satellite radar altimeters were observed to be 0.23 m, 0.25 m, and 0.26 m, respectively. The accuracy levels of the SSWS data products of the HY-2B/C/D satellite radar altimeters were observed to be 1.48 m/s, 1.59 m/s, and 1.35 m/s, respectively. Future research could further explore the differences and underlying reasons between the HY-2D and HY-2B satellite data and conduct more in-depth analyses to improve the quality and accuracy of the data. Furthermore, the validation of HY-2C/D satellites' altimeter data could be based on the comparison with altimeter data from other satellites, such as Sentinel-3(A, B).

In previous studies, satellite data quality assessment has been limited to the evaluation of altimetry parameters, while the assessment of satellite altimetry data coverage has been neglected. Altimetry parameters evaluation typically focuses on the accuracy and precision of the SSH and SLA information provided by satellite radar altimeters to ensure their reliability. However, this assessment methodology does not fully take into account the spatial coverage of satellite data. Coverage assessment of satellite altimetry data is critical for many applications. For example, in the prediction and evaluation of ocean circulation and sea surface wind fields, if satellite altimetry data only covers a limited area or a specific geographical area, it cannot provide comprehensive information, thus limiting the accuracy and reliability of relevant research. Therefore, in order to assess more fully the quality of satellite radar altimeter data, the coverage of satellite altimetry data must be taken into account. The results of this study also prove the scientific design of the orbit of China's first dynamic environment satellite constellation.

The minimum radius of HY-2B/C/D three satellites to find the observation point in the global ocean surface shrank from 471.13 km to 90.33 km in the 14-day cycle. This study evaluated the observation efficiency of China's first dynamic environment satellite constellation, as well as of the six other satellite networks. The findings demonstrated that, when compared to the six satellites from other countries, the observation efficiency of the HY-2B, HY-2C, and HY2D satellite networks was roughly comparable. This will provide an effective scientific basis for the accurate observation of ocean surface temperature, sea surface salinity, sea surface wind field, waves, surface current field, and other elements of the ocean dynamic environment.

After the completion of China's first dynamic environment satellite constellation, the satellite radar altimeter obtained SWH as well as SSWS, but also in the global coastal wave disaster monitoring, it played an important role. Combining the altimeter data from other satellites, as well as the future planned satellite constellation of microwave remote sensing technology for detecting the ocean dynamic environment, will achieve higher accuracy in the calculation of SLA, SWH, SSWS, and other parameters, providing large amount of data services for ocean remote sensing, contributing to global ocean governance, and addressing climate change.

Author Contributions: Conceptualization, D.Q. and Y.J.; methodology, S.L.; validation, D.Q. and Y.J.; formal analysis, M.L. and Y.J.; writing—original draft preparation, Y.J. and S.L.; writing—review and editing, D.Q. and Y.J.; visualization, M.L. All authors have read and agreed to the published version of the manuscript.

Funding: This research was funded by the National Natural Science Foundation of China (No. 42192561, No. 42192531).

Data Availability Statement: Data underlying the results presented in this paper are not publicly available at this time but may be obtained from the authors upon reasonable request.

Acknowledgments: The authors thank the reviewers and editors for their positive and constructive comments, which have significantly improved the work.

Conflicts of Interest: The authors declare no conflict of interest. The funders had no role in the design of the study; in the collection, analyses, or interpretation of data; in the writing of the manuscript; or in the decision to publish the results.

References

1. Jia, Y.; Yang, J.; Lin, M.; Zhang, Y.; Ma, C.; Fan, C. Global Assessments of the HY-2B Measurements and Cross-Calibrations with Jason-3. *Remote Sens.* **2020**, *12*, 2470. [CrossRef]
2. Jia, Y.; Lin, M.; Zhang, Y. Evaluations of the Significant Wave Height Products of HY-2B Satellite Radar Altimeters. *Mar. Geod.* **2020**, *43*, 396–413. [CrossRef]
3. Perbos, J.; Escudier, P.; Parisot, F.; Zaouche, G.; Vincent, P.; Menard, Y.; Manon, F.; Kunstmann, G.; Royer, D.; Fu, L.L. Jason-1: Assessment of the System Performances Special Issue: Jason-1 Calibration/Validation. *Mar. Geod.* **2003**, *26*, 147–157. [CrossRef]
4. Vincent, P.; Desai, S.D.; Dorandeu, J.; Ablain, M.; Soussi, B.; Callahan, P.S.; Haines, B.J. Jason-1 Geophysical Performance Evaluation Special Issue: Jason-1 Calibration/Validation. *Mar. Geod.* **2003**, *26*, 167–186. [CrossRef]
5. Dorandeu, J.; Ablain, M.; Faugere, Y.; Mertz, F.; Soussi, B.; Vincent, P. Jason-1 global statistical evaluation and performance assessment: Calibration and cross-calibration results. *Mar. Geod.* **2004**, *27*, 345–372. [CrossRef]
6. Faugere, Y.; Dorandeu, J.; Lefevre, F.; Picot, N.; Femenias, P. Envisat Ocean Altimetry Performance Assessment and Cross-calibration. *Sensors* **2006**, *6*, 100–130. [CrossRef]
7. Prandi, P.; Philipps, S.; Pignot, V.; Picot, N. SARAL/AltiKa Global Statistical Assessment and Cross-Calibration with Jason-2. *Mar. Geod.* **2015**, *38*, 297–312. [CrossRef]
8. Dettmering, D.; Schwatke, C.; Bosch, W. Global Calibration of SARAL/AltiKa Using Multi-Mission Sea Surface Height Crossovers. *Mar. Geod.* **2015**, *38*, 206–218. [CrossRef]
9. Meng, J.; Yu, F.; Zhuang, Z.; Qi, J.; Chen, G. Quality analysis of sea level height data of HY-2C satellite. *Haiyang Xuebao* **2022**, *44*, 173–181.
10. Yang, S.; Zhang, L.; Lin, M.; Zou, J.; Mu, B.; Peng, H. Evaluation of Sea Surface Wind Products from Scatterometer Onboard the Chinese HY-2D Satellite. *Remote Sens.* **2023**, *15*, 852. [CrossRef]
11. Zieger, S.; Babanin, A.V.; Erick Rogers, W.; Young, I.R. Observation-based source terms in the third-generation wave model WAVEWATCH. *Ocean Model.* **2015**, *96*, 2–25. [CrossRef]
12. Gower, J.F.R. Inter-calibration of wave and wind data from TOPEX/POSEIDON and moored buoys off the west coast of Canada. *J. Geophys. Res.* **1996**, *101*, 3817–3829. [CrossRef]
13. Dobson, E.; Monaldo, F.; Goldhirsh, J.; Wilkerson, J. Validation of Geosat altimeter-derived wind speeds and significant wave height using buoy data. *J. Geophys. Res.* **1987**, *92*, 10719–10731. [CrossRef]
14. Young, I.R.; Sanina, E.; Babanin, A.V. Calibration and Cross Validation of a Global Wind and Wave Database of Altimeter, Radiometer, and Scatterometer Measurements. *J. Atmos. Ocean. Technol.* **2017**, *34*, 1285–1306. [CrossRef]
15. Yang, J.; Zhang, J.; Wang, C. Sentinel-3A SRAL Global Statistical Assessment and Cross-Calibration with Jason-3. *Remote Sens.* **2019**, *11*, 1573. [CrossRef]
16. Carter, D.J.T.; Challenor, P.G.; Srokosz, M.A. An assessment of Geosat wave height and wind speed measurements. *J. Geophys. Res.* **1992**, *97*, 11383–11392. [CrossRef]
17. Brown, G. The average impulse response of a rough surface and its applications. *IEEE Tran. Antennas Propag.* **1977**, *25*, 67–74. [CrossRef]
18. Fedor, L.S.; Godbey, T.W.; Gower, J.F.R.; Guptill, R.; Hayne, G.S.; Rufenach, C.L.; Walsh, E.J. Satellite altimeter measurements of sea state-An algorithm comparison. *J. Geophys. Res.* **1979**, *84*, 3991–4001. [CrossRef]
19. Amarouche, L.; Thibaut, P.; Zanife, O.Z.; Dumont, J.P.; Vincent, P.; Steunou, N. Improving the Jason-1 Ground Retracking to Better Account for Attitude Effects. *Mar. Geod.* **2004**, *27*, 171–197. [CrossRef]
20. Bosch, W.; Dettmering, D.; Schwatke, C. Multi-Mission Cross-Calibration of Satellite Altimeters: Constructing a Long-Term Data Record for Global and Regional Sea Level Change Studies. *Remote Sens.* **2014**, *6*, 2255–2281. [CrossRef]
21. Bao, L.; Gao, P.; Peng, H.; Jia, Y.; Shum, C.K.; Lin, M.; Guo, Q. First accuracy assessment of the HY-2A altimeter sea surface height observations: Cross-calibration results. *Adv. Space Res.* **2015**, *55*, 90–105. [CrossRef]
22. Sepulveda, H.H.; Queffeulou, P.; Ardhuin, F. Assessment of SARAL/AltiKa Wave Height Measurements Relative to Buoy, Jason-2, and Cryosat-2 Data. *Mar. Geod.* **2015**, *38*, 449–465. [CrossRef]
23. Ribal, A.; Young, I.R. 33 years of globally calibrated wave height and wind speed data based on altimeter observations. *Sci. Data* **2019**, *6*, 77. [CrossRef] [PubMed]
24. Ablain, M.; Philipps, S.; Picot, N.; Bronner, E. Jason-2 Global Statistical Assessment and Cross-Calibration with Jason-1. *Mar. Geod.* **2010**, *33*, 162–185. [CrossRef]
25. Rodriguez, E.; Chapman, B. Extracting ocean surface information from altimeter returns: The deconvolution method. *J. Geophys. Res.* **1989**, *94*, 9761–9778. [CrossRef]
26. Hayne, G. Radar altimeter mean return waveforms from near-normal-incidence ocean surface scattering. *IEEE Tran. Antennas Propag.* **1980**, *28*, 687–692. [CrossRef]
27. Callahan, P.S.; Rodriguez, E. Retracking of Jason-1 data. *Mar. Geod.* **2004**, *27*, 391–407. [CrossRef]

28. Zhao, D.; Li, S.; Song, C. The comparison of altimeter retrieval algorithms of the wind speed and the wave period. *Acta Oceanol. Sin.* **2012**, *31*, 1–9. [CrossRef]
29. Vinoth, J.; Young, I.R. Global Estimates of Extreme Wind Speed and Wave Height. *J. Clim.* **2011**, *24*, 1647–1665. [CrossRef]
30. Young, I.R.; Babanin, A.V.; Zieger, S. Response to Comment on "Global Trends in Wind Speed and Wave Height". *Science* **2011**, *334*, 905. [CrossRef]
31. Queffeulou, P. Long-Term Validation of Wave Height Measurements from Altimeters. *Mar. Geod.* **2004**, *27*, 495–510. [CrossRef]
32. Durrant, T.H.; Greenslade, D.J.M.; Simmonds, I. Validation of Jason-1 and Envisat Remotely Sensed Wave Heights. *J. Atmos. Ocean. Technol.* **2009**, *26*, 123–134. [CrossRef]
33. Passaro, M.; Fenoglio-Marc, L.; Cipollini, P. Validation of Significant Wave Height From Improved Satellite Altimetry in the German Bight. *IEEE Tran. Geosci. Remote* **2015**, *53*, 2146–2156. [CrossRef]
34. Monaldo, F. Expected differences between buoy and radar altimeter estimates of wind speed and significant wave height and their implications on buoy-altimeter comparisons. *J. Geophys. Res.* **1988**, *93*, 2285–2302. [CrossRef]
35. Wang, J.; Aouf, L.; Jia, Y.; Zhang, Y. Validation and Calibration of Significant Wave Height and Wind Speed Retrievals from HY2B Altimeter Based on Deep Learning. *Remote Sens.* **2020**, *12*, 2858. [CrossRef]
36. Young, I.R. Seasonal variability of the global ocean wind and wave climate. *Int. J. Climatol.* **1999**, *19*, 931–950. [CrossRef]